

Natural Adversarial Examples

Dan Hendrycks
UC Berkeley

hendrycks@berkeley.edu

Kevin Zhao*
University of Washington

kwzhao@cs.washington.edu

Steven Basart*
University of Chicago
steven@ttic.edu

Jacob Steinhardt
UC Berkeley
jsteinhardt@berkeley.edu

Dawn Song
UC Berkeley
dawnsong@berkeley.edu

Abstract

We introduce natural adversarial examples—real-world, unmodified, and naturally occurring examples that cause machine learning model performance to substantially degrade. We introduce two new datasets of natural adversarial examples. The first dataset contains 7,500 natural adversarial examples for ImageNet classifiers and serves as a hard ImageNet classier test set called IMAGENET-A. We also curate an adversarial out-of-distribution detection dataset called IMAGENET-O, which to our knowledge is the first out-of-distribution detection dataset created for ImageNet models. These two datasets provide new ways to measure model robustness and uncertainty. Like ℓ_p adversarial examples, our natural adversarial examples transfer to unseen black-box models. For example, on IMAGENET-A a DenseNet-121 obtains around 2% accuracy, an accuracy drop of approximately 90%, and its out-of-distribution detection performance on IMAGENET-O is near random chance levels. Popular training techniques for improving robustness have little effect, but some architectural changes provide mild improvements. Future research is required to enable generalization to natural adversarial examples.

1. Introduction

Research on the ImageNet [12] benchmark has led to numerous advances in classification [31], object detection [29], and segmentation [19]. ImageNet classification improvements are broadly applicable and highly predictive of improvements on many tasks [30]. Improvements on ImageNet classification have been so great that some call ImageNet classifiers “superhuman” [21]. However, performance is decidedly subhuman when the test distribution does not match the training distribution [22]. The distribution

*Equal Contribution.

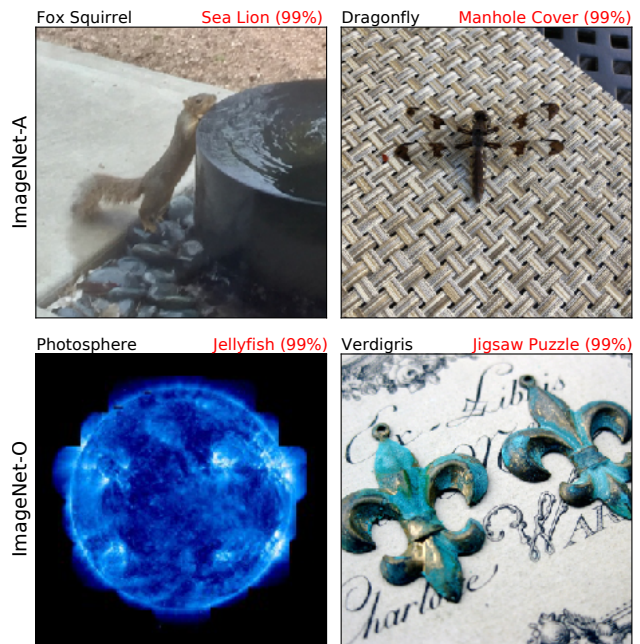


Figure 1: Natural adversarial examples from IMAGENET-A and IMAGENET-O. The black text is the actual class, and the red text is a ResNet-50 prediction and its confidence. IMAGENET-A contains images that classifiers should be able to classify, while IMAGENET-O contains anomalies of unforeseen classes which should result in low-confidence predictions. ImageNet-1K models do not train on examples from “Photosphere” nor “Verdigris” classes, so these images are anomalous. Many natural adversarial examples lead to wrong predictions, despite having no adversarial modifications as they are examples which occur naturally.

seen at test-time can include inclement weather conditions and obscured objects, and it can also include objects that are anomalous. Recht et al., 2019 [39] remind us that ImageNet test examples tend to be simple, clear, close-up images, so that the current test set may be too easy and not represent

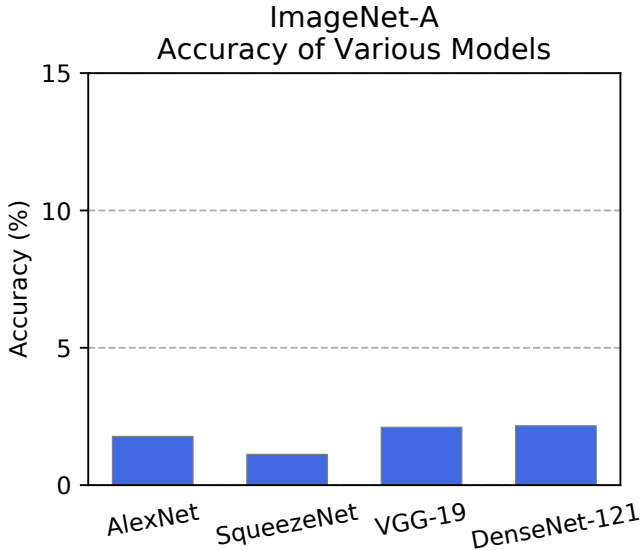


Figure 2: For most of the natural adversarial examples from IMAGENET-A, various ImageNet classifiers of different architectures fail to generalize.

harder images encountered in the real world.

Real-world images may be chosen adversarially to cause performance decline. Goodfellow et al., 2017 [17] define adversarial examples [45] as “inputs to machine learning models that an attacker has intentionally designed to cause the model to make a mistake.” Adversarial examples enable measuring worst-case model performance. Our aim is to measure worst-case performance while requiring that examples are naturally occurring. Most adversarial examples research centers around artificial ℓ_p adversarial examples, which are examples perturbed by nearly worst-case distortions that are small in an ℓ_p sense. Aside from the known difficulties in evaluating ℓ_p robustness correctly [9, 8], Gilmer et al., 2018 [16] point out that ℓ_p adversarial examples assume an unrealistic threat model because attackers are often free to choose any desired input. Consequently, if an attacker aims to subvert black-box classifier accuracy, they could mimic known errors [16]. Attackers can reliably and easily create black-box attacks by exploiting these consistent natural model errors, and thus carefully applying gradient perturbations to create an attack is unnecessary. This less restricted threat model has been discussed but not explored thoroughly until now.

We adversarially curate two hard ImageNet test sets of *natural adversarial examples* (NAEs). These images are natural, unmodified, real-world examples and are selected to cause a fixed model to make a mistake, as with synthetic adversarial examples. The first dataset allows us to test model classification performance when the input data distribution shifts. We call this dataset IMAGENET-A, which contains images from a distribution unlike the ImageNet

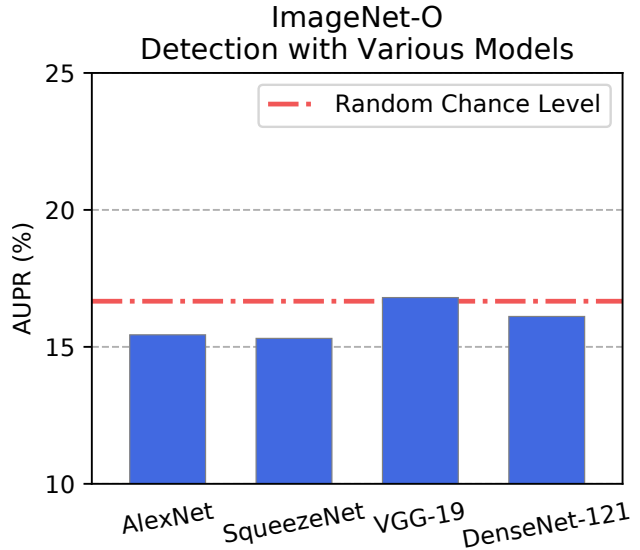


Figure 3: IMAGENET-O out-of-distribution detection performance. Higher AUPR is better. See Section 5 for a description of the AUPR. These ImageNet models assign high confidence predictions to out-of-class samples from IMAGENET-O, hence the AUPR is low. Usually the model confidence is higher on in-distribution examples and lower on out-of-distribution examples, but IMAGENET-O examples are frequently ascribed higher confidence than in-distribution examples.

training distribution. IMAGENET-A examples belong to ImageNet classes, but the examples are harder. They cause consistent classification mistakes due to scene complications encountered in the long tail of scene configurations and by exploiting classifier blind spots (see Section 4).

The second dataset allows us to test model uncertainty estimates when semantic factors of the data distribution shift. Our second dataset of NAEs is IMAGENET-O, which contains image concepts from outside ImageNet-1K. These out-of-distribution NAEs reliably cause models to mistake the examples as high-confidence in-distribution examples. To our knowledge this is the first dataset of anomalies or out-of-distribution examples developed to test ImageNet models. Some natural adversarial examples are depicted in Figure 1. While IMAGENET-A enables us to test image classification performance when the input data distribution shifts, IMAGENET-O enables us to test out-of-distribution detection performance when the label distribution shifts.

We examine methods to improve performance on natural adversarial examples. However, this is difficult because Figure 2 and Figure 3 show that NAEs successfully transfer to unseen or black-box models. As with other black-box adversarial examples, natural adversarial examples are selected to break a fixed model, in this case ResNet-50, but they transfer reliably to new and

black-box models. To improve robustness, numerous techniques have been proposed. Of these, Stylized ImageNet data augmentation [14] and ℓ_∞ adversarial training hardly increase robustness to natural adversarial examples. However, greater performance gains follow from architectural modifications, as we show in Section 5. Even so, current models have substantial room for improvement. Code and our two challenging datasets are available at github.com/hendrycks/natural-adv-examples.

2. Related Work

Adversarial Examples. Adversarial examples are a means to estimate worst-case model performance. While we aim to estimate the worst-case accuracy in natural settings, most work studies ℓ_p adversarial attacks [36]. Several other forms of adversarial attacks have been considered in the literature, including elastic deformations [47], adversarial coloring [4, 26], and synthesis via generative models [3, 43] and evolutionary search [38], among others. Other work has shown how to print 2D [34, 7] or 3D [41, 2] objects that fool classifiers. These existing adversarial attacks are all based on synthesized images or objects, and some have questioned whether they provide a reliable window into real-world robustness [16]. Our examples are closer in spirit to the hypothetical adversarial photographer discussed in [6], and by definition these adversarial photos occur in the real world.

Adversarial examples can also be thought of as examples resulting from forms of hard example mining [44]. For instance, ℓ_p adversarial examples are found or mined with SGD, and the resulting noise perturbations are among the hardest within an ℓ_p ball. Our datasets can be construed as a collection of hard, real examples that are carefully mined or curated. Parallel work [13, 50] in natural language processing constructs datasets by way of adversarial filtration. They collect examples which fool a model, and use these examples to fool other models. Like this parallel research, we also use adversarial filtration, but the technique of adversarial filtration has not been applied to image tasks until this paper.

Robustness to Shifted Input Distributions. Recht et al., 2019 [39] create a new ImageNet test set resembling the original test set as closely as possible. They found evidence that matching the difficulty of the original test set required selecting images deemed the easiest and most obvious by Mechanical Turkers. IMAGENET-A helps measure generalization to harder scenarios. Brendel et al., 2019 [5] show that classifiers that do not know the spatial ordering of image regions can be competitive on the ImageNet test set, possibly due to the dataset’s lack of difficulty. Judging classifiers by their performance on easier examples has potentially masked many of their shortcomings. For example, Geirhos et al., 2019 [14] artificially overwrite each ImageNet image’s textures and conclude that classifiers learn to rely on textu-

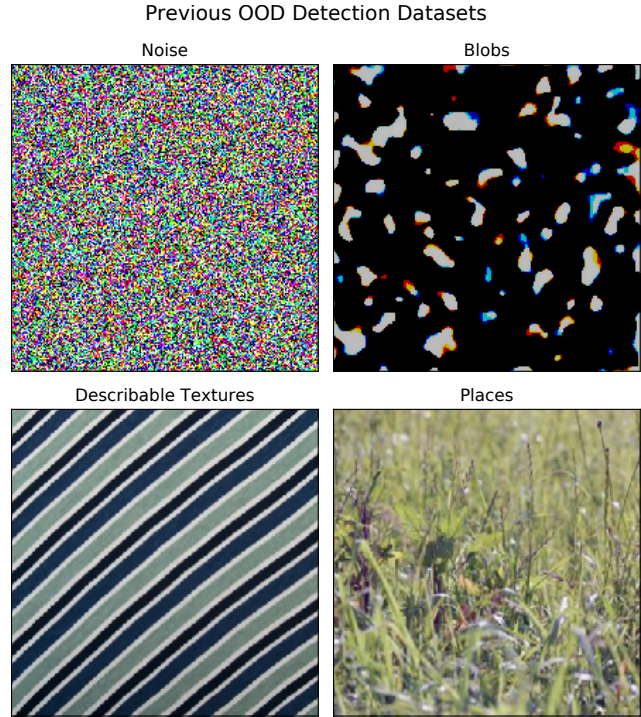


Figure 4: Previous work on out-of-distribution (OOD) detection uses synthetic anomalies and anomalies from wholly different data generating processes. For instance, previous work uses Bernoulli noise, blobs, the Describable Textures Dataset [11], and Places365 scenes [52] to test ImageNet out-of-distribution detectors. To our knowledge we propose the first dataset of out-of-distribution examples collected for ImageNet models. In our dataset, low-level image statistics are similar to ImageNet-1K’s low-level statistics since the data generating process is similar to ImageNet-1K.

ral cues and under-utilize information about object shape. Recent work shows that classifiers are highly susceptible to non-adversarial stochastic corruptions [22]. While they distort images with 75 different algorithmically generated corruptions, our sources of distribution shift tend to be more heterogeneous, varied, and realistic. Obtaining robustness to varied forms of distribution shift is difficult. For example, previous works train on various distortions and show that networks tend to memorize distortions and thereby fail to generalize to new and unseen distortions [46, 15]. Hence, robustly generalizing to unseen long-tail complications, such as obfuscating translucent shrink wrap which envelopes a toaster, could also be difficult.

Out-of-Distribution Detection. OOD detection [23, 35, 24, 25] is a nascent subfield that lacks agreed-upon evaluation schemes. Generally, models learn a distribution, such as the ImageNet-1K distribution, and are tasked with producing quality anomaly scores that distinguish between usual test set examples and examples from held-out anomalous



Figure 5: Additional natural adversarial examples from the IMAGENET-A dataset. Examples are adversarially selected to cause classifier accuracy to degrade. The black text is the actual class, and the red text is a ResNet-50 prediction.



Figure 6: Additional natural adversarial examples from the IMAGENET-O dataset. Examples are adversarially selected to cause out-of-distribution detection performance to degrade. Examples do not belong to ImageNet classes, and they are wrongly assigned highly confident predictions. The black text is the actual class, and the red text is a ResNet-50 prediction and the prediction confidence.

distributions. For instance, Hendrycks et al., 2017 [23] treat CIFAR-10 as the in-distribution and treat Gaussian noise and the SUN scene dataset [49] as out-of-distribution data. That paper also shows that the negative of the maximum softmax probability, or the the negative of the classifier prediction probability, is a high-performing anomaly score that can separate in- and out-of-distribution examples, so much so that it remains competitive to this day. Since that time, other works on out-of-distribution detection continue to use datasets from other research benchmarks as stand-ins for out-of-distribution datasets. For example, some use the datasets shown in Figure 4 as out-of-distribution datasets [24]. However, many of these anomaly sources are unnatural and deviate in numerous ways from the distribution of usual examples [1]. In fact, some of the distributions can be deemed anomalous from local image statistics alone. Meinke et al., 2019 [37] propose studying adversarial out-of-distribution detection by detecting adversarially optimized uniform noise. In contrast, we propose a dataset for more realistic adversarial anomaly detection; our dataset contains hard anomalies generated by shifting the distribution’s labels and keeping non-semantic factors similar to the in-distribution.

3. The Design and Construction of IMAGENET-A and IMAGENET-O

IMAGENET-A is a dataset of natural adversarial examples for ImageNet classifiers, or real-world examples that fool current classifiers. We sample natural images from the real world, rather than sampling adversarial synthetic images from the range of a generative model [43] or from an ℓ_p ball [42]. To find natural adversarial examples, we first download numerous images related to an ImageNet class. Thereafter we delete the images that ResNet-50 [20] classifiers correctly predict. With the remaining incorrectly classified images, we manually select a subset of high-quality images to create IMAGENET-A.

Next, IMAGENET-O is a dataset of natural adversarial examples for ImageNet out-of-distribution detectors. To create this dataset, we download ImageNet-22K and delete examples from ImageNet-1K. With the remaining ImageNet-22K examples that do not belong to ImageNet-1K classes, we keep examples that are classified by a ResNet-50 as an ImageNet-1K class with high confidence. Then we manually select a subset of high-quality images. Both datasets were manually labelled by graduate students over several months.

Dataset	Task	Examples	Data Sources
IMAGENET-A	Classification	7,500	iNaturalist, Flickr, DuckDuckGo
IMAGENET-O	Out-of-Distribution Detection	2,000	ImageNet-22K excluding ImageNet-1K

Table 1: Descriptions of our two natural adversarial examples datasets. IMAGENET-A tests ImageNet classifier accuracy when the input data distribution shifts, and IMAGENET-O tests out-of-distribution detection performance when the label distribution shifts. Both datasets are comprised of difficult natural adversarial examples. More details are in Section 3.

This process is explicated below.

IMAGENET-A Class Restrictions. We select a 200-class subset of ImageNet-1K’s 1,000 classes so that errors among these 200 classes would be considered egregious [12]. For instance, wrongly classifying Norwich terriers as Norfolk terriers does less to demonstrate faults in current classifiers than mistaking a Persian cat for a candle. We additionally avoid rare classes such as “snow leopard,” classes that have changed much since 2012 such as “iPod,” coarse classes such as “spiral,” classes that are often image backdrops such as “valley,” and finally classes that tend to overlap such as “honeycomb,” “bee,” “bee house,” and “bee eater”; “eraser,” “pencil sharpener” and “pencil case”; “sink,” “medicine cabinet,” “pill bottle” and “band-aid”; and so on. The 200 IMAGENET-A classes cover most broad categories spanned by ImageNet-1K; see the Supplementary Materials for the full class list.

IMAGENET-O Class Restrictions. We again select a 200-class subset of ImageNet-1K’s 1,000 classes. These 200 classes determine the in-distribution or the distribution that is considered usual. As before, the 200 classes cover most broad categories spanned by ImageNet-1K; see the Supplementary Materials for the full class list.

IMAGENET-A Data Aggregation. Curating a large set of natural adversarial examples requires combing through an even larger set of images. Fortunately, the website iNaturalist has millions of user-labeled images of animals, and Flickr has even more user-tagged images of objects. We download images related to each of the 200 ImageNet classes by leveraging user-provided labels and tags. After exporting or scraping data from sites including iNaturalist, Flickr, and DuckDuckGo, we adversarially select images by removing examples that fail to fool our ResNet-50 models. Of the remaining images, we select low-confidence images and then ensure each image is valid through human review. For this procedure to work, many images are necessary; if we only used the original ImageNet test set as a source rather than iNaturalist, Flickr, and DuckDuckGo, some classes would have zero images after the first round of filtration.

For concreteness, we describe the selection process for the dragonfly class. We download 81,413 dragonfly images from iNaturalist, and after performing a basic filter we have 8,925 dragonfly images. In the algorithmically suggested shortlist, 1,452 images remain. From this shortlist, 80 dragonfly images are manually selected, but hundreds more

could be chosen. Hence for just one class we may review over 1,000 images.

We now describe this process more exactly. We use ResNet-50s for filtering, one pre-trained on ImageNet-1K then fine-tuned on the 200 class subset, and one pre-trained on ImageNet-1K where 200 of its 1,000 logits are used in classification. Both classifiers have similar accuracy on the 200 clean test set classes from ImageNet-1K. The ResNet-50s perform 10-crop classification of each image, and should any crop be classified correctly by the ResNet-50s, the image is removed. If either ResNet-50 assigns greater than 15% confidence to the correct class, the image is also removed; this is done so that natural adversarial examples yield misclassifications with low confidence in the correct class, like in untargeted adversarial attacks. Now, some classification confusions are greatly over-represented, such as Persian cat and lynx. We would like IMAGENET-A to have great variability in its types of errors and cause classifiers to have a dense confusion matrix. Consequently, we perform a second round of filtering to create a shortlist where each confusion only appears at most 15 times. Finally, we manually select images from this shortlist in order to ensure IMAGENET-A images are simultaneously valid, single-class, and high-quality. In all, the IMAGENET-A dataset has 7,500 natural adversarial examples. Additional IMAGENET-A images are in Figure 5.

IMAGENET-O Data Aggregation. Our dataset for adversarial out-of-distribution detection is created by fooling a ResNet-50 out-of-distribution detector. The negative of the prediction confidence of a ResNet-50 ImageNet classifier serves as our anomaly score [23]. Usually in-distribution examples produce higher confidence predictions than OOD examples, but we curate OOD examples that have high confidence predictions. To gather candidate natural adversarial examples, we use the ImageNet-22K dataset with ImageNet-1K classes deleted. We choose the ImageNet-22K dataset since it was collected in the same way as ImageNet-1K. ImageNet-22K allows us to have coverage of numerous visual concepts and vary the distribution’s semantics without unnatural or unwanted non-semantic data shift. After excluding ImageNet-1K images, we process the remaining ImageNet-22K images and keep the images which cause the ResNet-50 to have high confidence, or a low anomaly score. We then manually select a high-quality subset of the remaining images to create IMAGENET-O. We suggest only training models with



Figure 7: Natural adversarial examples from IMAGENET-A demonstrating classifier failure modes. For instance, classifiers may use erroneous background cues for prediction. Further description of these failure modes is in Section 4.

data from the 1,000 ImageNet-1K classes, since the dataset becomes trivial if models train on ImageNet-22K. To our knowledge, this dataset is the first anomalous dataset curated for ImageNet models and enables researchers to study adversarial out-of-distribution detection. In all, the IMAGENET-O dataset has 2,000 natural adversarial examples. Additional example IMAGENET-O images are in Figure 6.

4. Illustrative Classifier Failure Modes

The natural adversarial examples in IMAGENET-A uncover numerous failure modes of modern convolutional neural networks. We describe our findings after having viewed tens of thousands of candidate natural adversarial examples. Some of these failure modes may also explain poor IMAGENET-O performance, but for simplicity we describe our observations with IMAGENET-A examples.

Figure 7 shows that classifiers may predict a class even when the image does not contain the subparts necessary to identify the predicted class. In the leftmost image of Figure 7, the candle is predicted as a jack-o'-lantern with 99.94% confidence, despite the absence of a pumpkin or carved faces. Networks may also rely too heavily on color and texture, for instance misclassifying a dragonfly as a skunk due to its white and black colors. Since classifiers are taught to associate entire images with an object class, frequently appearing background elements may also become associated with a class, such as wood being associated with nails. Other examples include classifiers heavily associating hummingbird feeders with hummingbirds, leaf-covered tree branches being associated with the white-headed capuchin monkey class, snow being associated with shovels, and dumpsters with garbage trucks.

Classifiers also demonstrate fickleness to small scene variations. The center pane of Figure 7 shows an American alligator swimming. With different frames, the classifier prediction varies erratically between classes that are semantically loose and separate. For other images of the swimming alligator, classifiers predict that the alligator is a cliff, lynx, and a fox squirrel. In the final pane, we find that the classifiers overgeneralize shadows to sundials, tricycles to bicycles and circles, digital clocks to keyboards and calculators, and so on. Current convolutional networks have pervasive and diverse failure modes that can now be estimated with IMAGENET-A.

5. Experiments

Metrics. Our metric for assessing robustness to natural adversarial examples for classifiers is the top-1 accuracy on IMAGENET-A. For reference, the top-1 accuracy on the 200 IMAGENET-A classes using usual ImageNet images is usually $\geq 90\%$ for ordinary classifiers. Next, our metric for assessing out-of-distribution detection performance of NAEs is the area under the precision-recall curve (AUPR). This metric requires anomaly scores. Our anomaly score is the negative of the maximum softmax probabilities [23] from a model that can classify the 200 IMAGENET-O classes specified in Section 3. We collect anomaly scores with the ImageNet validation examples for the said 200 classes. Then, we collect anomaly scores for the IMAGENET-O examples. Higher performing OOD detectors would assign IMAGENET-O examples lower confidences, or higher anomaly scores. With these anomaly scores, we can compute the area under the precision-recall curve [40]. Random chance levels for the AUPR is approximately 16.67% with IMAGENET-O, and

the highest possible AUPR is 100%.

5.1. Robust Training Methods Hardly Help

We examine popular robust training techniques. Unfortunately, we find that on natural adversarial examples for classifiers, these techniques hardly help. In this section we exclude IMAGENET-O results, as the robust training methods hardly help with out-of-distribution detection as well.

ℓ_∞ **Adversarial Training.** We investigate how much robustness ℓ_∞ adversarial training confers, so we shall first describe ℓ_∞ adversarial training, and then adversarially train ResNeXts. Adversarially training the parameters θ with loss function L on dataset \mathcal{D} involves the objective

$$\min_{\theta} \mathbb{E}_{(x,y) \sim \mathcal{D}} \left[\max_{x' \in S} L(x', y; \theta) \right]$$

where $S = \{x' : \|x - x'\|_\infty < \varepsilon\}$.

The maximization over $x' \in S$ is approximated through an iterative procedure similar to projected gradient ascent [36],

$$x^{t+1} = \Pi_{x+S} (x^t + \alpha \text{sign}(\nabla_x L(x, y; \theta))) .$$

We try three different adversarial training schemes with adversaries of different strengths. The first is degenerate adversarial training with a zero-step adversary. In the zero-step case, training examples are simply perturbed by randomly scaled uniform noise where the noise strength for each example is $\varepsilon = 8/255 \times u$, $u \sim \mathcal{U}[0, 1]$, so that ε varies between examples. We randomly scale epsilon so that the model learns to be robust to perturbations of various scales. The second is FGSM training against a single-step adversary. Here $\varepsilon = \alpha = 8/255 \times u$, $u \sim \mathcal{U}[0, 1]$. Finally, we adversarially train against a 10-step PGD attacker with $\varepsilon = 8/255 \times u$, $u \sim \mathcal{U}[0, 1]$, and $\alpha = \varepsilon/\sqrt{10}$.

We train a ResNeXt-50 (32x4d) [48] from scratch on the 200 ImageNet-1K classes appearing in IMAGENET-A. This network trains for 90 epochs. The first five epochs follow a linear warmup learning rate schedule [18], and the learning rate drops by a factor of 0.1 at epochs 30, 60, and 80. We use a batch size of 256, a maximum learning rate of 0.1, a momentum parameter of 0.9, and a weight decay strength of 10^{-4} . We use standard random horizontal flipping and cropping where each image is of size $224 \times 224 \times 3$.

Observe in Figure 8 that augmenting the training data with random uniform noise slightly improves robustness (2.13% over 1.31%). Adding noise from a 1-step FGSM adversary slightly increases robustness further (2.28%). A stronger 10-step ℓ_∞ adversary imparts slightly greater IMAGENET-A robustness (2.69%). However, the model trained on clean data has 89.22% accuracy on the 200 class subset of ImageNet-1K’s test set, while uniform noise data augmentation corresponds to an accuracy of 88.93%, FGSM to 83.95%, and PGD to 81.88%. Thus ℓ_∞ adversarial training’s accuracy gains are hardly worth the cost.

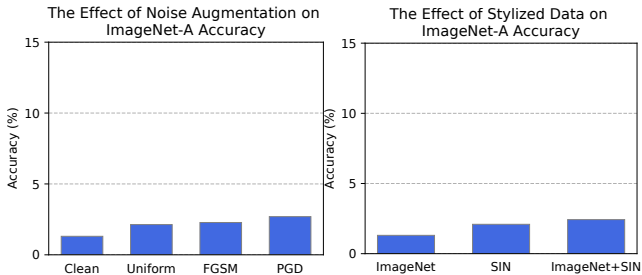


Figure 8: Adversarially training a ResNeXt-50 against uniform noise, 1-step (FGSM) and 10-step (PGD) ℓ_∞ adversaries slightly improves accuracy on natural adversarial examples. Training a ResNeXt-50 on Stylized ImageNet (SIN) and both ImageNet and SIN together slightly improves accuracy.

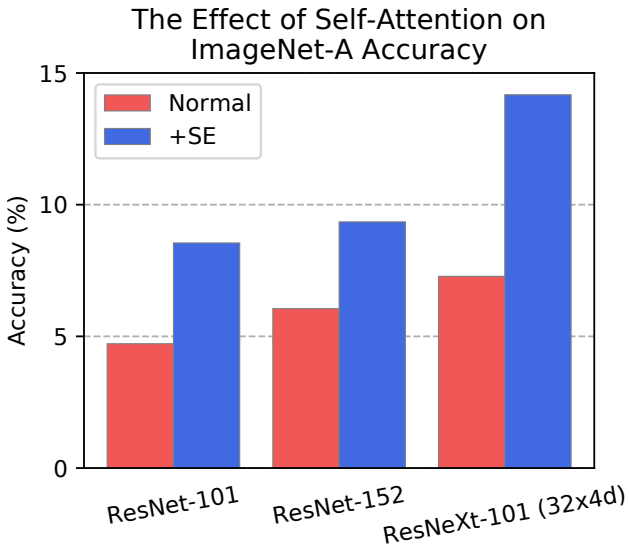


Figure 9: Applying self-attention in the form of Squeeze-and-Excitation (SE) can improve IMAGENET-A accuracy.

Stylized ImageNet Augmentation. In Figure 7, we observe that classifiers may rely too heavily on color and textural features. Geirhos et al., 2019 [14] propose making networks rely less on texture by training classifiers on images where textures are transferred from art pieces. They accomplish this by applying style transfer to ImageNet training images to create a dataset they call Stylized ImageNet or SIN for short. We test whether training with SIN images can improve IMAGENET-A robustness.

Reducing a ResNeXt-50’s texture bias by training with SIN images does little to improve IMAGENET-A accuracy. For reference, the ResNeXt-50 trained on ImageNet images obtains 89.22% top-1 accuracy on the 200 class subset of ImageNet-1K’s test set. If we train a ResNeXt-50 entirely on Stylized ImageNet images, the top-1 accuracy on ImageNet-1K’s 200 class test set is a meager 65.87%, while its accuracy on IMAGENET-A only increases from 1.31% to

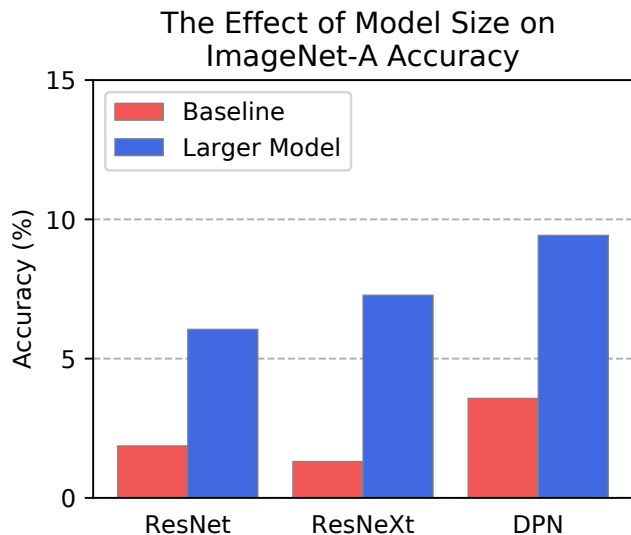


Figure 10: Increasing the capacity of ResNets, Dual-PathNetworks [10], and ResNeXts improves accuracy on IMAGENET-A. We show the performance of a ResNet-34, ResNet-152, ResNeXt-50 (32×4d), ResNeXt-101 (64×4d), DPN-68, and DPN-98.

2.09}. This demonstrates that natural adversarial examples can successfully transfer to unseen models trained on different data. As shown in Figure 8, data augmentation with Stylized ImageNet results in minor accuracy improvements.

5.2. Architectural Changes Can Help

Self-Attention. Convolutional neural networks with self-attention [27] are designed to better capture long-range dependencies and interactions across an image. Self-attention helps GANs learn how to generate images with plausible shape [51], and in classification, self-attention is utilized in state-of-the-art ImageNet-1K models. We consider the self-attention technique called Squeeze-and-Excitation (SE) [28], which won the final ImageNet competition in 2017. While integrating Squeeze-and-Excitation into a ResNeXt-101 (32×4d) improves top-1 accuracy on the 200 class subset of ImageNet-1K by less than 1%, SE improves IMAGENET-A accuracy by approximately 10%. However, performance improvements are minor on IMAGENET-O. For example, a ResNet-152’s AUPR increases from 17.2% to 17.9%.

Size. Simply increasing the width and number of layers of a network is sufficient to automatically impart more IMAGENET-A accuracy and IMAGENET-O OOD detection performance. Increasing network capacity has been shown to improve performance on ℓ_p adversarial examples [33], common corruptions [22], and now also on natural adversarial examples as demonstrated in Figure 10 and Figure 11. The ResNet-34’s top-1 accuracy and AUPR is 1.9% and 16.0%, respectively, while the ResNet-152 obtains 6.1% top-1 accuracy and 18.0% AUPR. The

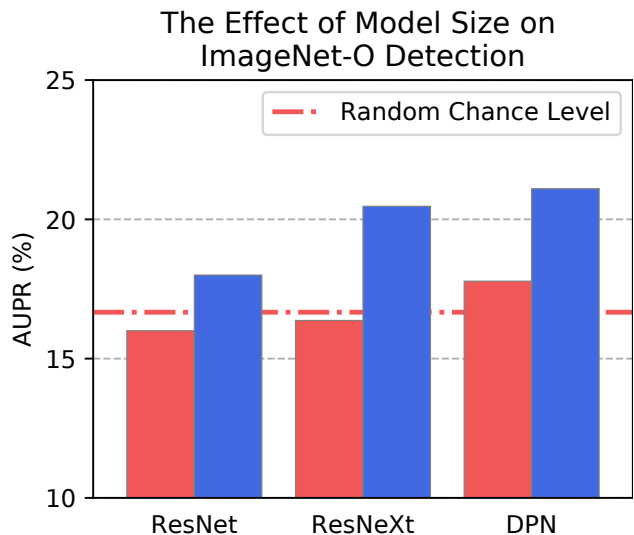


Figure 11: Increasing the capacity of ResNets, ResNeXts, and DualPathNetworks also improves adversarial out-of-distribution detection performance on IMAGENET-O.

ResNeXt-50 (32×4d)’s top-1 accuracy and AUPR is 1.3% and 16.4%, respectively, while the ResNeXt-101 (64×4d) obtains 7.3% top-1 accuracy and 20.5% AUPR. The DualPathNetwork-68’s top-1 accuracy and AUPR is 3.6% and 17.8%, respectively, while the ResNeXt-101 (64×4d) obtains 9.4% top-1 accuracy and 21.1% AUPR. This demonstrates the progress is possible on natural adversarial examples, but there is much room for improvement.

6. Conclusion

In this paper, we introduced natural adversarial examples for classifiers and out-of-distribution detectors. Our IMAGENET-A dataset contains 7,500 examples and reliably degrades classification accuracy. Likewise, IMAGENET-O natural adversarial examples reliably degrade ImageNet out-of-distribution detection performance. IMAGENET-O enables the measurement of adversarial out-of-distribution detection, and is the first out-of-distribution detection dataset collected for ImageNet models. Both of our novel datasets allow us to measure model reliability under input and label distribution shifts. These naturally occurring images expose common blindspots of current convolutional networks, and solving these tasks will require addressing long-standing but under-explored failure modes of current models such as over-reliance on texture, over-generalization, and more. We found that these failures are only slightly less pronounced with different training regimes and architectures, but performance is still low. In this work, we introduce two new and difficult ImageNet test sets to measure model performance under distribution shift—an important research aim as computer vision systems are deployed in increasingly precarious environments.

References

- [1] Faruk Ahmed and Aaron C. Courville. Detecting semantic anomalies. *ArXiv*, abs/1908.04388, 2019.
- [2] Anish Athalye, Logan Engstrom, Andrew Ilyas, and Kevin Kwok. Synthesizing robust adversarial examples. *arXiv preprint arXiv:1707.07397*, 2017.
- [3] Shumeet Baluja and Ian Fischer. Adversarial transformation networks: Learning to generate adversarial examples. *CoRR*, abs/1703.09387, 2017.
- [4] Anand Bhattad, Min Jin Chong, Kaizhao Liang, Bo Li, and David A. Forsyth. Big but imperceptible adversarial perturbations via semantic manipulation. *CoRR*, abs/1904.06347, 2019.
- [5] Wieland Brendel and Matthias Bethge. Approximating cnns with bag-of-local-features models works surprisingly well on imagenet. *CoRR*, abs/1904.00760, 2018.
- [6] Tom B. Brown, Nicholas Carlini, Chiyuan Zhang, Catherine Olsson, Paul Francis Christiano, and Ian J. Goodfellow. Unrestricted adversarial examples. *CoRR*, abs/1809.08352, 2018.
- [7] Tom B Brown, Dandelion Mané, Aurko Roy, Martín Abadi, and Justin Gilmer. Adversarial patch. *arXiv preprint arXiv:1712.09665*, 2017.
- [8] Nicholas Carlini, Anish Athalye, Nicolas Papernot, Wieland Brendel, Jonas Rauber, Dimitris Tsipras, Ian Goodfellow, Aleksander Madry, and Alexey Kurakin. On evaluating adversarial robustness. *arXiv pre-print*, 2019.
- [9] Nicholas Carlini and David Wagner. Adversarial examples are not easily detected: Bypassing ten detection methods, 2017.
- [10] Yunpeng Chen, Jianan Li, Huaxin Xiao, Xiaojie Jin, Shuicheng Yan, and Jiashi Feng. Dual path networks. In *NIPS*, 2017.
- [11] Mircea Cimpoi, Subhansu Maji, Iasonas Kokkinos, Sammy Mohamed, and Andrea Vedaldi. Describing textures in the wild. *Computer Vision and Pattern Recognition*, 2014.
- [12] Jia Deng, Wei Dong, Richard Socher, Li jia Li, Kai Li, and Li Fei-Fei. ImageNet: A large-scale hierarchical image database. *CVPR*, 2009.
- [13] Dheeru Dua, Yizhong Wang, Pradeep Dasigi, Gabriel Stanovsky, Sameer Singh, and Matt Gardner. Drop: A reading comprehension benchmark requiring discrete reasoning over paragraphs. In *NAACL-HLT*, 2019.
- [14] Robert Geirhos, Patricia Rubisch, Claudio Michaelis, Matthias Bethge, Felix A Wichmann, and Wieland Brendel. Imagenet-trained cnns are biased towards texture; increasing shape bias improves accuracy and robustness. *ICLR*, 2019.
- [15] Robert Geirhos, Carlos R. M. Temme, Jonas Rauber, Heiko H. Schütt, Matthias Bethge, and Felix A. Wichmann. Generalisation in humans and deep neural networks. *NeurIPS*, 2018.
- [16] Justin Gilmer, Ryan P. Adams, Ian J. Goodfellow, David Andersen, and George E. Dahl. Motivating the rules of the game for adversarial example research. *CoRR*, abs/1807.06732, 2018.
- [17] Ian Goodfellow, Nicolas Papernot, Sandy Huang, Yan Duan, , and Peter Abbeel. Attacking machine learning with adversarial examples. *OpenAI Blog*, 2017.
- [18] Priya Goyal, Piotr Dollár, Ross B. Girshick, Pieter Noordhuis, Lukasz Wesolowski, Aapo Kyrola, Andrew Tulloch, Yangqing Jia, and Kaiming He. Accurate, large minibatch SGD: Training imagenet in 1 hour. *CoRR*, abs/1706.02677, 2017.
- [19] Kaiming He, Georgia Gkioxari, Piotr Dollár, and Ross B. Girshick. Mask r-cnn. In *CVPR*, 2018.
- [20] Kaiming He, Xiangyu Zhang, Shaoqing Ren, and Jian Sun. Deep residual learning for image recognition. *CVPR*, 2015.
- [21] Kaiming He, Xiangyu Zhang, Shaoqing Ren, and Jian Sun. Delving deep into rectifiers: Surpassing human-level performance on imagenet classification. *2015 IEEE International Conference on Computer Vision (ICCV)*, pages 1026–1034, 2015.
- [22] Dan Hendrycks and Thomas Dietterich. Benchmarking neural network robustness to common corruptions and perturbations. *ICLR*, 2019.
- [23] Dan Hendrycks and Kevin Gimpel. A baseline for detecting misclassified and out-of-distribution examples in neural networks. *ICLR*, 2017.
- [24] Dan Hendrycks, Mantas Mazeika, and Thomas Dietterich. Deep anomaly detection with outlier exposure. *ICLR*, 2019.
- [25] Dan Hendrycks, Mantas Mazeika, Saurav Kadavath, and Dawn Song. Using self-supervised learning can improve model robustness and uncertainty. *Advances in Neural Information Processing Systems (NeurIPS)*, 2019.
- [26] Hossein Hosseini and Radha Poovendran. Semantic adversarial examples. *2018 IEEE/CVF Conference on Computer Vision and Pattern Recognition Workshops (CVPRW)*, pages 1695–16955, 2018.
- [27] Jie Hu, Li Shen, Samuel Albanie, Gang Sun, and Andrea Vedaldi. Gather-excite : Exploiting feature context in convolutional neural networks. In *NeurIPS*, 2018.
- [28] Jie Hu, Li Shen, and Gang Sun. Squeeze-and-excitation networks. *2018 IEEE/CVF Conference on Computer Vision and Pattern Recognition*, 2018.
- [29] Jonathan Huang, Vivek Rathod, Chen Sun, Menglong Zhu, Anoop Korattikara Balan, Alireza Fathi, Ian Fischer, Zbigniew Wojna, Yang Song, Sergio Guadarrama, and Kevin Murphy. Speed/accuracy trade-offs for modern convolutional object detectors. *2017 IEEE Conference on Computer Vision and Pattern Recognition (CVPR)*, 2017.
- [30] Simon Kornblith, Jonathon Shlens, and Quoc V. Le. Do better imagenet models transfer better? *CoRR*, abs/1805.08974, 2018.
- [31] Alex Krizhevsky, Ilya Sutskever, and Geoffrey E Hinton. ImageNet classification with deep convolutional neural networks. *NIPS*, 2012.
- [32] A. Kumar, P. Liang, and T. Ma. Verified uncertainty calibration. In *Advances in Neural Information Processing Systems (NeurIPS)*, 2019.
- [33] Alexey Kurakin, Ian Goodfellow, and Samy Bengio. Adversarial machine learning at scale. *ICLR*, 2017.
- [34] Alexey Kurakin, Ian J. Goodfellow, and Samy Bengio. Adversarial examples in the physical world. *CoRR*, abs/1607.02533, 2017.

- [35] Kimin Lee, Honglak Lee, Kibok Lee, and Jinwoo Shin. Training confidence-calibrated classifiers for detecting out-of-distribution samples. *ICLR*, 2018.
- [36] Aleksander Madry, Aleksandar Makelov, Ludwig Schmidt, Dimitris Tsipras, and Adrian Vladu. Towards deep learning models resistant to adversarial attacks. *ICLR*, 2018.
- [37] Alexander Meinke and Matthias Hein. Towards neural networks that provably know when they don’t know. *ArXiv*, abs/1909.12180, 2019.
- [38] Anh Mai Nguyen, Jason Yosinski, and Jeff Clune. Deep neural networks are easily fooled: High confidence predictions for unrecognizable images. *2015 IEEE Conference on Computer Vision and Pattern Recognition (CVPR)*, pages 427–436, 2015.
- [39] Benjamin Recht, Rebecca Roelofs, Ludwig Schmidt, and Vaishal Shankar. Do imagenet classifiers generalize to imagenet? *ArXiv*, abs/1902.10811, 2019.
- [40] Takaya Saito and Marc Rehmsmeier. The precision-recall plot is more informative than the ROC plot when evaluating binary classifiers on imbalanced datasets. In *PLoS ONE*. 2015.
- [41] Mahmood Sharif, Sruti Bhagavatula, Lujio Bauer, and Michael K Reiter. Accessorize to a crime: Real and stealthy attacks on state-of-the-art face recognition. In *Proceedings of the 2016 ACM SIGSAC Conference on Computer and Communications Security*, pages 1528–1540. ACM, 2016.
- [42] Yash Sharma and Pin-Yu Chen. Attacking the Madry defense model with l_1 -based adversarial examples. *ICLR Workshop*, 2018.
- [43] Yang Song, Rui Shu, Nate Kushman, and Stefano Ermon. Constructing unrestricted adversarial examples with generative models. In *NeurIPS*, 2018.
- [44] Kah Kay Sung. Learning and example selection for object and pattern detection. 1995.
- [45] Christian Szegedy, Wojciech Zaremba, Ilya Sutskever, Joan Bruna, Dumitru Erhan, Ian Goodfellow, and Rob Fergus. Intriguing properties of neural networks, 2014.
- [46] Igor Vasiljevic, Ayan Chakrabarti, and Gregory Shakhnarovich. Examining the impact of blur on recognition by convolutional networks, 2016.
- [47] Chaowei Xiao, Jun-Yan Zhu, Bo Li, Warren He, Mingyan Liu, and Dawn Xiaodong Song. Spatially transformed adversarial examples. *CoRR*, abs/1801.02612, 2018.
- [48] Saining Xie, Ross Girshick, Piotr Dollár, Zhuowen Tu, and Kaiming He. Aggregated residual transformations for deep neural networks. *CVPR*, 2016.
- [49] Jian xiong Xiao, James Hays, Krista A. Ehinger, Aude Oliva, and Antonio Torralba. Sun database: Large-scale scene recognition from abbey to zoo. *2010 IEEE Computer Society Conference on Computer Vision and Pattern Recognition*, pages 3485–3492, 2010.
- [50] Rowan Zellers, Ari Holtzman, Yonatan Bisk, Ali Farhadi, and Yejin Choi. Hellaswag: Can a machine really finish your sentence? In *ACL*, 2019.
- [51] Han Zhang, Ian J. Goodfellow, Dimitris N. Metaxas, and Augustus Odena. Self-attention generative adversarial networks. *CoRR*, abs/1805.08318, 2018.
- [52] Bolei Zhou, Agata Lapedriza, Aditya Khosla, Aude Oliva, and Antonio Torralba. Places: A 10 million image database for scene recognition. *PAMI*, 2017.

A. IMAGENET-A Classes

The 200 ImageNet classes that we selected for IMAGENET-A are as follows.

‘Stingray,’ ‘goldfinch, *Carduelis carduelis*,’ ‘junco, snowbird,’ ‘robin, American robin, *Turdus migratorius*,’ ‘jay,’ ‘bald eagle, American eagle, *Haliaeetus leucocephalus*,’ ‘vulture,’ ‘eft,’ ‘bullfrog, *Rana catesbeiana*,’ ‘box turtle, box tortoise,’ ‘common iguana, iguana, *Iguana iguana*,’ ‘agama,’ ‘African chameleon, *Chamaeleo chamaeleon*,’ ‘American alligator, *Alligator mississippiensis*,’ ‘garter snake, grass snake,’ ‘harvestman, daddy longlegs, *Phalangium opilio*,’ ‘scorpion,’ ‘tarantula,’ ‘centipede,’ ‘sulphur-crested cockatoo, *Kakatoe galerita*, *Cacatua galerita*,’ ‘lorikeet,’ ‘hummingbird,’ ‘toucan,’ ‘drake,’ ‘goose,’ ‘koala, koala bear, kangaroo bear, native bear, *Phascolarctos cinereus*,’ ‘jellyfish,’ ‘sea anemone, anemone,’ ‘flatworm, platyhelminth,’ ‘snail,’ ‘crayfish, crawfish, crawdad, crawdaddy,’ ‘hermit crab,’ ‘flamingo,’ ‘American egret, great white heron, *Egretta albus*,’ ‘oystercatcher, oyster catcher,’ ‘pelican,’ ‘sea lion,’ ‘Chihuahua,’ ‘golden retriever,’ ‘Rottweiler,’ ‘German shepherd, German shepherd dog, German police dog, alsatian,’ ‘pug, pug-dog,’ ‘red fox, *Vulpes vulpes*,’ ‘Persian cat,’ ‘lynx, catamount,’ ‘lion, king of beasts, *Panthera leo*,’ ‘American black bear, black bear, *Ursus americanus*, *Euarctos americanus*,’ ‘mongoose,’ ‘ladybug, ladybeetle, lady beetle, ladybird, ladybird beetle,’ ‘rhinoceros beetle,’ ‘weevil,’ ‘fly,’ ‘bee,’ ‘ant, emmet, pismire,’ ‘grasshopper, hopper,’ ‘walking stick, walkingstick, stick insect,’ ‘cockroach, roach,’ ‘mantis, mantid,’ ‘leafhopper,’ ‘dragonfly, darning needle, devil’s darning needle, sewing needle, snake feeder, snake doctor, mosquito hawk, skeeter hawk,’ ‘monarch, monarch butterfly, milkweed butterfly, *Danaus plexippus*,’ ‘cabbage butterfly,’ ‘lycaenid, lycaenid butterfly,’ ‘starfish, sea star,’ ‘wood rabbit, cottontail, cottontail rabbit,’ ‘porcupine, hedgehog,’ ‘fox squirrel, eastern fox squirrel, *Sciurus niger*,’ ‘marmot,’ ‘bison,’ ‘skunk, polecat, wood pussy,’ ‘armadillo,’ ‘baboon,’ ‘capuchin, ringtail, *Cebus capucinus*,’ ‘African elephant, *Loxodonta africana*,’ ‘puffer, pufferfish, blowfish, globefish,’ ‘academic gown, academic robe, judge’s robe,’ ‘accordion, piano accordion, squeeze box,’ ‘acoustic guitar,’ ‘airliner,’ ‘ambulance,’ ‘apron,’ ‘balance beam, beam,’ ‘balloon,’ ‘banjo,’ ‘barn,’ ‘barrow, garden cart, lawn cart, wheelbarrow,’ ‘basketball,’ ‘beacon, lighthouse, beacon light, pharos,’ ‘beaker,’ ‘bikini, two-piece,’ ‘bow,’ ‘bow tie, bow-tie, bowtie,’ ‘breastplate, aegis, egis,’ ‘broom,’ ‘candle, taper, wax light,’ ‘canoe,’ ‘castle,’ ‘cello, violoncello,’ ‘chain,’ ‘chest,’ ‘Christmas stocking,’ ‘cowboy boot,’ ‘cradle,’ ‘dial telephone, dial phone,’ ‘digital clock,’ ‘doormat, welcome mat,’ ‘drumstick,’ ‘dumbbell,’ ‘envelope,’ ‘feather boa, boa,’ ‘flagpole, flagstaff,’ ‘forklift,’ ‘fountain,’ ‘garbage truck, dustcart,’ ‘goblet,’ ‘go-kart,’ ‘golf cart, golf cart,’ ‘grand piano, grand,’ ‘hand blower, blow dryer, blow drier, hair dryer, hair drier,’ ‘iron, smooth-

ing iron,’ ‘jack-o’-lantern,’ ‘jeep, landrover,’ ‘kimono,’ ‘lighter, light, igniter, ignitor,’ ‘limousine, limo,’ ‘manhole cover,’ ‘maraca,’ ‘marimba, xylophone,’ ‘mask,’ ‘mitten,’ ‘mosque,’ ‘nail,’ ‘obelisk,’ ‘ocarina, sweet potato,’ ‘organ, pipe organ,’ ‘parachute, chute,’ ‘parking meter,’ ‘piggy bank, penny bank,’ ‘pool table, billiard table, snooker table,’ ‘puck, hockey puck,’ ‘quill, quill pen,’ ‘racket, racquet,’ ‘reel,’ ‘revolver, six-gun, six-shooter,’ ‘rocking chair, rocker,’ ‘rugby ball,’ ‘saltshaker, salt shaker,’ ‘sandal,’ ‘sax, saxophone,’ ‘school bus,’ ‘schooner,’ ‘sewing machine,’ ‘shovel,’ ‘sleeping bag,’ ‘snowmobile,’ ‘snowplow, snowplough,’ ‘soap dispenser,’ ‘spatula,’ ‘spider web, spider’s web,’ ‘steam locomotive,’ ‘stethoscope,’ ‘studio couch, day bed,’ ‘submarine, pigboat, sub, U-boat,’ ‘sundial,’ ‘suspension bridge,’ ‘syringe,’ ‘tank, army tank, armored combat vehicle, armoured combat vehicle,’ ‘teddy, teddy bear,’ ‘toaster,’ ‘torch,’ ‘tricycle, trike, velocipede,’ ‘umbrella,’ ‘unicycle, monocycle,’ ‘viaduct,’ ‘volleyball,’ ‘washer, automatic washer, washing machine,’ ‘water tower,’ ‘wine bottle,’ ‘wreck,’ ‘guacamole,’ ‘pretzel,’ ‘cheeseburger,’ ‘hotdog, hot dog, red hot,’ ‘broccoli,’ ‘cucumber, cuke,’ ‘bell pepper,’ ‘mushroom,’ ‘lemon,’ ‘banana,’ ‘custard apple,’ ‘pomegranate,’ ‘carbonara,’ ‘bubble,’ ‘cliff, drop, drop-off,’ ‘volcano,’ ‘ballplayer, baseball player,’ ‘rapeseed,’ ‘yellow lady’s slipper, yellow lady-slipper, *Cypripedium calceolus*, *Cypripedium parviflorum*,’ ‘corn,’ ‘acorn.’

Their WordNet IDs are as follows.

n01498041,	n01531178,	n01534433,	n01558993,
n01580077,	n01614925,	n01616318,	n01631663,
n01641577,	n01669191,	n01677366,	n01687978,
n01694178,	n01698640,	n01735189,	n01770081,
n01770393,	n01774750,	n01784675,	n01819313,
n01820546,	n01833805,	n01843383,	n01847000,
n01855672,	n01882714,	n01910747,	n01914609,
n01924916,	n01944390,	n01985128,	n01986214,
n02007558,	n02009912,	n02037110,	n02051845,
n02077923,	n02085620,	n02099601,	n02106550,
n02106662,	n02110958,	n02119022,	n02123394,
n02127052,	n02129165,	n02133161,	n02137549,
n02165456,	n02174001,	n02177972,	n02190166,
n02206856,	n02219486,	n02226429,	n02231487,
n02233338,	n02236044,	n02259212,	n02268443,
n02279972,	n02280649,	n02281787,	n02317335,
n02325366,	n02346627,	n02356798,	n02361337,
n02410509,	n02445715,	n02454379,	n02486410,
n02492035,	n02504458,	n02655020,	n02669723,
n02672831,	n02676566,	n02690373,	n02701002,
n02730930,	n02777292,	n02782093,	n02787622,
n02793495,	n02797295,	n02802426,	n02814860,
n02815834,	n02837789,	n02879718,	n02883205,
n02895154,	n02906734,	n02948072,	n02951358,
n02980441,	n02992211,	n02999410,	n03014705,
n03026506,	n03124043,	n03125729,	n03187595,

n03196217, n03223299, n03250847, n03255030,
n03291819, n03325584, n03355925, n03384352,
n03388043, n03417042, n03443371, n03444034,
n03445924, n03452741, n03483316, n03584829,
n03590841, n03594945, n03617480, n03666591,
n03670208, n03717622, n03720891, n03721384,
n03724870, n03775071, n03788195, n03804744,
n03837869, n03840681, n03854065, n03888257,
n03891332, n03935335, n03982430, n04019541,
n04033901, n04039381, n04067472, n04086273,
n04099969, n04118538, n04131690, n04133789,
n04141076, n04146614, n04147183, n04179913,
n04208210, n04235860, n04252077, n04252225,
n04254120, n04270147, n04275548, n04310018,
n04317175, n04344873, n04347754, n04355338,
n04366367, n04376876, n04389033, n04399382,
n04442312, n04456115, n04482393, n04507155,
n04509417, n04532670, n04540053, n04554684,
n04562935, n04591713, n04606251, n07583066,
n07695742, n07697313, n07697537, n07714990,
n07718472, n07720875, n07734744, n07749582,
n07753592, n07760859, n07768694, n07831146,
n09229709, n09246464, n09472597, n09835506,
n11879895, n12057211, n12144580, n12267677.

B. IMAGENET-O Classes

The 200 ImageNet classes that we selected for IMAGENET-O are as follows.

‘goldfish, *Carassius auratus*;’ ‘triceratops;’ ‘harvestman, daddy longlegs, *Phalangium opilio*;’ ‘centipede;’ ‘sulphur-crested cockatoo, *Kakatoe galerita*, *Cacatua galerita*;’ ‘lorikeet;’ ‘jellyfish;’ ‘brain coral;’ ‘chambered nautilus, pearly nautilus, *nautilus*;’ ‘dugong, *Dugong dugon*;’ ‘starfish, sea star;’ ‘sea urchin;’ ‘hog, pig, grunter, squealer, *Sus scrofa*;’ ‘armadillo;’ ‘rock beauty, *Holocanthus tricolor*;’ ‘puffer, pufferfish, blowfish, globefish;’ ‘abacus;’ ‘accordion, piano accordion, squeeze box;’ ‘apron;’ ‘balance beam, beam;’ ‘ballpoint, ballpoint pen, ballpen, Biro;’ ‘Band Aid;’ ‘banjo;’ ‘barbershop;’ ‘bath towel;’ ‘bearskin, busby, shako;’ ‘binoculars, field glasses, opera glasses;’ ‘bolo tie, bolo, bola tie, bola;’ ‘bottlecap;’ ‘brassiere, bra, bandeau;’ ‘broom;’ ‘buckle;’ ‘bulletproof vest;’ ‘candle, taper, wax light;’ ‘car mirror;’ ‘chainlink fence;’ ‘chain saw, chainsaw;’ ‘chime, bell, gong;’ ‘Christmas stocking;’ ‘cinema, movie theater, movie theatre, movie house, picture palace;’ ‘combination lock;’ ‘corkscrew, bottle screw;’ ‘crane;’ ‘croquet ball;’ ‘dam, dike, dyke;’ ‘digital clock;’ ‘dishrag, dishcloth;’ ‘dogsled, dog sled, dog sleigh;’ ‘doormat, welcome mat;’ ‘drilling platform, offshore rig;’ ‘electric fan, blower;’ ‘envelope;’ ‘espresso maker;’ ‘face powder;’ ‘feather boa, boa;’ ‘fireboat;’ ‘fire screen, fireguard;’ ‘flute, transverse flute;’ ‘folding chair;’ ‘fountain;’ ‘fountain pen;’ ‘frying pan, frypan, skillet;’ ‘golf ball;’ ‘greenhouse, nursery, glasshouse;’

‘guillotine;’ ‘hamper;’ ‘hand blower, blow dryer, blow drier, hair dryer, hair drier;’ ‘harmonica, mouth organ, harp, mouth harp;’ ‘honeycomb;’ ‘hourglass;’ ‘iron, smoothing iron;’ ‘jack-o’-lantern;’ ‘jigsaw puzzle;’ ‘joystick;’ ‘lawn mower, mower;’ ‘library;’ ‘lighter, light, igniter, ignitor;’ ‘lipstick, lip rouge;’ ‘loupe, jeweler’s loupe;’ ‘magnetic compass;’ ‘manhole cover;’ ‘maraca;’ ‘marimba, xylophone;’ ‘mask;’ ‘matchstick;’ ‘maypole;’ ‘maze, labyrinth;’ ‘medicine chest, medicine cabinet;’ ‘mortar;’ ‘mosquito net;’ ‘mousetrap;’ ‘nail;’ ‘neck brace;’ ‘necklace;’ ‘nipple;’ ‘ocarina, sweet potato;’ ‘oil filter;’ ‘organ, pipe organ;’ ‘oscilloscope, scope, cathode-ray oscilloscope, CRO;’ ‘oxygen mask;’ ‘paddle-wheel, paddle wheel;’ ‘panpipe, pandean pipe, syrinx;’ ‘park bench;’ ‘pencil sharpener;’ ‘Petri dish;’ ‘pick, plectrum, plectron;’ ‘picket fence, paling;’ ‘pill bottle;’ ‘ping-pong ball;’ ‘pinwheel;’ ‘plate rack;’ ‘plunger, plumber’s helper;’ ‘pool table, billiard table, snooker table;’ ‘pot, flowerpot;’ ‘power drill;’ ‘prayer rug, prayer mat;’ ‘prison, prison house;’ ‘punching bag, punch bag, punching ball, punchball;’ ‘quill, quill pen;’ ‘radiator;’ ‘reel;’ ‘remote control, remote;’ ‘rubber eraser, rubber, pencil eraser;’ ‘rule, ruler;’ ‘safe;’ ‘safety pin;’ ‘saltshaker, salt shaker;’ ‘scale, weighing machine;’ ‘screw;’ ‘screwdriver;’ ‘shoji;’ ‘shopping cart;’ ‘shower cap;’ ‘shower curtain;’ ‘ski;’ ‘sleeping bag;’ ‘slot, one-armed bandit;’ ‘snowmobile;’ ‘soap dispenser;’ ‘solar dish, solar collector, solar furnace;’ ‘space heater;’ ‘spatula;’ ‘spider web, spider’s web;’ ‘stove;’ ‘strainer;’ ‘stretcher;’ ‘submarine, pigboat, sub, U-boat;’ ‘swimming trunks, bathing trunks;’ ‘swing;’ ‘switch, electric switch, electrical switch;’ ‘syringe;’ ‘tennis ball;’ ‘thatch, thatched roof;’ ‘theater curtain, theatre curtain;’ ‘thimble;’ ‘throne;’ ‘tile roof;’ ‘toaster;’ ‘tricycle, trike, velocipede;’ ‘turnstile;’ ‘umbrella;’ ‘vending machine;’ ‘waffle iron;’ ‘washer, automatic washer, washing machine;’ ‘water bottle;’ ‘water tower;’ ‘whistle;’ ‘Windsor tie;’ ‘wooden spoon;’ ‘wool, woolen, woollen;’ ‘crossword puzzle, crossword;’ ‘traffic light, traffic signal, stoplight;’ ‘ice lolly, lolly, lollipop, popsicle;’ ‘bagel, beigel;’ ‘pretzel;’ ‘hotdog, hot dog, red hot;’ ‘mashed potato;’ ‘broccoli;’ ‘cauliflower;’ ‘zucchini, courgette;’ ‘acorn squash;’ ‘cucumber, cuke;’ ‘bell pepper;’ ‘Granny Smith;’ ‘strawberry;’ ‘orange;’ ‘lemon;’ ‘pineapple, ananas;’ ‘banana;’ ‘jackfruit, jak, jack;’ ‘pomegranate;’ ‘chocolate sauce, chocolate syrup;’ ‘meat loaf, meatloaf;’ ‘pizza, pizza pie;’ ‘burrito;’ ‘bubble;’ ‘volcano;’ ‘corn;’ ‘acorn;’ ‘hen-of-the-woods, hen of the woods, *Polyporus frondosus*, *Grifola frondosa*.’

Their WordNet IDs are as follows.

n01443537, n01704323, n01770081, n01784675,
n01819313, n01820546, n01910747, n01917289,
n01968897, n02074367, n02317335, n02319095,
n02395406, n02454379, n02606052, n02655020,
n02666196, n02672831, n02730930, n02777292,
n02783161, n02786058, n02787622, n02791270,
n02808304, n02817516, n02841315, n02865351,

n02877765,	n02892767,	n02906734,	n02910353,
n02916936,	n02948072,	n02965783,	n03000134,
n03000684,	n03017168,	n03026506,	n03032252,
n03075370,	n03109150,	n03126707,	n03134739,
n03160309,	n03196217,	n03207743,	n03218198,
n03223299,	n03240683,	n03271574,	n03291819,
n03297495,	n03314780,	n03325584,	n03344393,
n03347037,	n03372029,	n03376595,	n03388043,
n03388183,	n03400231,	n03445777,	n03457902,
n03467068,	n03482405,	n03483316,	n03494278,
n03530642,	n03544143,	n03584829,	n03590841,
n03598930,	n03602883,	n03649909,	n03661043,
n03666591,	n03676483,	n03692522,	n03706229,
n03717622,	n03720891,	n03721384,	n03724870,
n03729826,	n03733131,	n03733281,	n03742115,
n03786901,	n03788365,	n03794056,	n03804744,
n03814639,	n03814906,	n03825788,	n03840681,
n03843555,	n03854065,	n03857828,	n03868863,
n03874293,	n03884397,	n03891251,	n03908714,
n03920288,	n03929660,	n03930313,	n03937543,
n03942813,	n03944341,	n03961711,	n03970156,
n03982430,	n03991062,	n03995372,	n03998194,
n04005630,	n04023962,	n04033901,	n04040759,
n04067472,	n04074963,	n04116512,	n04118776,
n04125021,	n04127249,	n04131690,	n04141975,
n04153751,	n04154565,	n04201297,	n04204347,
n04209133,	n04209239,	n04228054,	n04235860,
n04243546,	n04252077,	n04254120,	n04258138,
n04265275,	n04270147,	n04275548,	n04330267,
n04332243,	n04336792,	n04347754,	n04371430,
n04371774,	n04372370,	n04376876,	n04409515,
n04417672,	n04418357,	n04423845,	n04429376,
n04435653,	n04442312,	n04482393,	n04501370,
n04507155,	n04525305,	n04542943,	n04554684,
n04557648,	n04562935,	n04579432,	n04591157,
n04597913,	n04599235,	n06785654,	n06874185,
n07615774,	n07693725,	n07695742,	n07697537,
n07711569,	n07714990,	n07715103,	n07716358,
n07717410,	n07718472,	n07720875,	n07742313,
n07745940,	n07747607,	n07749582,	n07753275,
n07753592,	n07754684,	n07768694,	n07836838,
n07871810,	n07873807,	n07880968,	n09229709,
n09472597,	n12144580,	n12267677,	n13052670.

C. Color Counterfactuals

In Figure 7, we claim that models are sensitive to color. The counterfactual in Figure 12 corroborates this claim.

D. IMAGENET-A Calibration

In this section we show IMAGENET-A calibration results. **Uncertainty Metrics.** The ℓ_2 Calibration Error is how we measure miscalibration. We would like classifiers that



Figure 12: A demonstration of color sensitivity. While the leftmost image is classified as “banana,” the images with modified color are correctly classified.

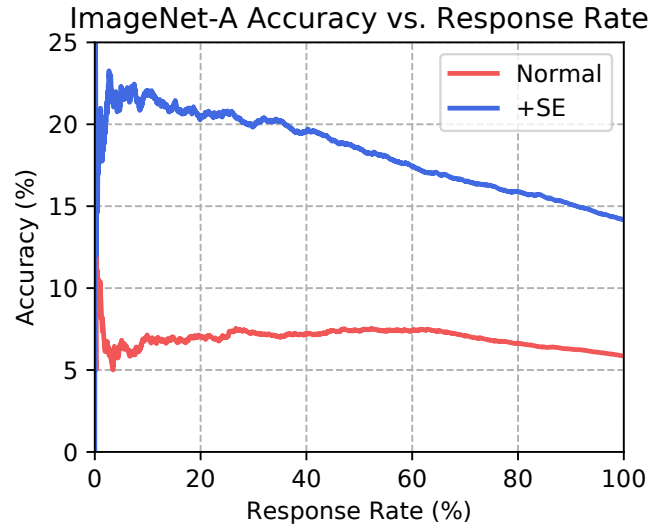


Figure 13: The Response Rate Accuracy curve for a ResNeXt-101 (32×4d) with and without Squeeze-and-Excitation (SE). The Response Rate is the percent classified. The accuracy at a $n\%$ response rate is the accuracy on the $n\%$ of examples where the classifier is most confident.

can reliably forecast their accuracy. Concretely, we want classifiers which give examples 60% confidence to be correct 60% of the time. We judge a classifier’s miscalibration with the ℓ_2 Calibration Error [32].

Our second uncertainty estimation metric is the *Area Under the Response Rate Accuracy Curve (AURRA)*. Responding only when confident is often preferable to predicting falsely. In these experiments, we allow classifiers to respond to a subset of the test set and abstain from predicting the rest. Classifiers with quality uncertainty estimates should be capable identifying examples it is likely to predict falsely and abstain. If a classifier is required to abstain from predicting on 90% of the test set, or equivalently respond to the remaining 10% of the test set, then we should like the classifier’s uncertainty estimates to separate correctly and falsely classified examples and have high accuracy on the

selected 10%. At a fixed response rate, we should like the accuracy to be as high as possible. At a 100% response rate, the classifier accuracy is the usual test set accuracy. We vary the response rates and compute the corresponding accuracies to obtain the Response Rate Accuracy (RRA) curve. The area under the Response Rate Accuracy curve is the AURRA. To compute the AURRA in this paper, we use the maximum softmax probability. For response rate p , we take the p fraction of examples with highest maximum softmax probability. If the response rate is 10%, we select the top 10% of examples with the highest confidence and compute the accuracy on these examples. An example RRA curve is in Figure 13.

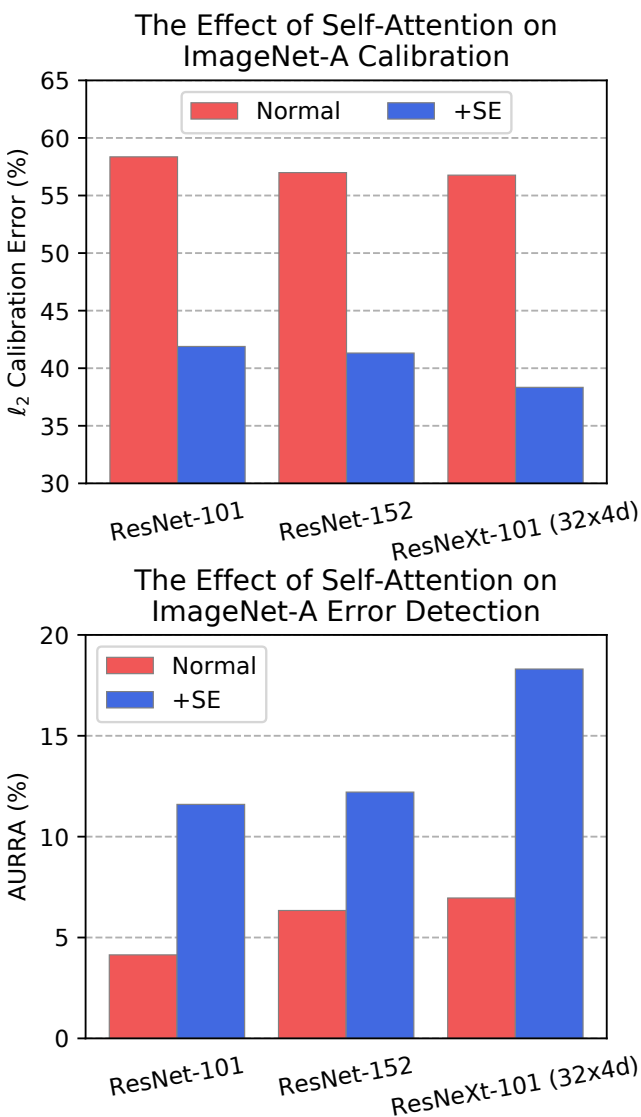


Figure 14: Self-attention’s influence on IMAGENET-A ℓ_2 calibration and error detection.

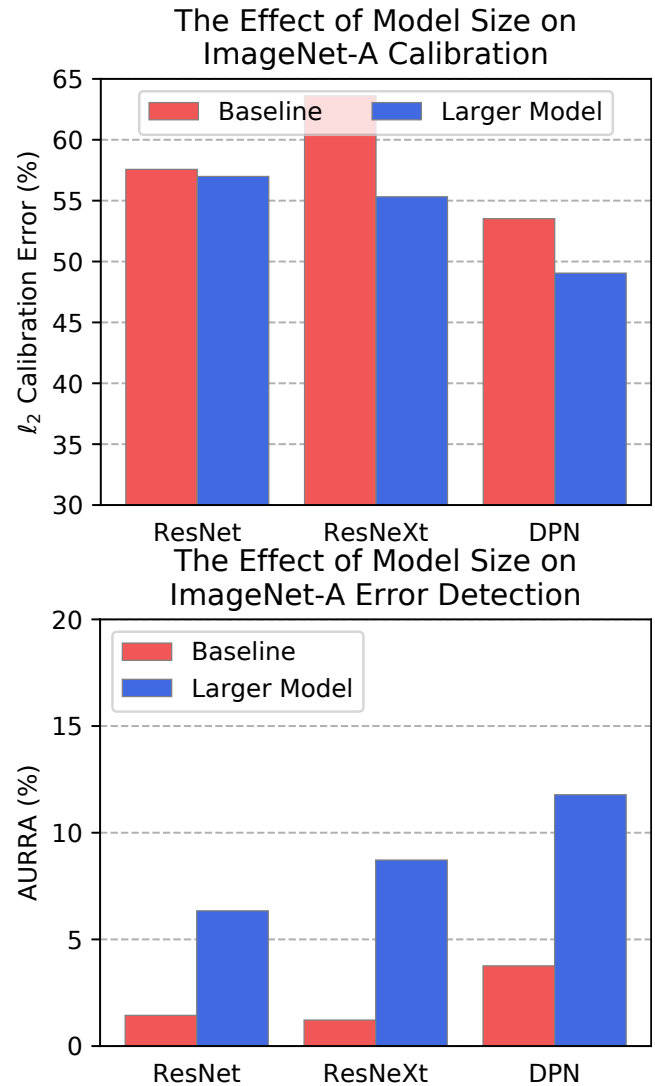


Figure 15: Model size’s influence on IMAGENET-A ℓ_2 calibration and error detection.